

1 Relationships between kinematic characteristics and ratio of forces during initial sprint
2 acceleration

3

4 Daniel King¹, Louise Burnie², Ryu Nagahara³, Neil E Bezodis¹

5

6 ¹ Applied Sports, Technology, Exercise and Medicine Research Centre, Swansea University,
7 Bay Campus, Crymlyn Burrows, SA1 8EN, UK.

8 ² Department of Sport, Exercise and Rehabilitation, Northumbria University, Newcastle upon
9 Tyne, NE1 8ST, UK.

10 ³ National Institute of Fitness and Sports in Kanoya, 1 Shiromizu-cho, Kanoya, Kagoshima
11 891-2393, Japan.

12

13 Corresponding Author: Neil Bezodis (n.e.bezodis@swansea.ac.uk)

14

15 ORCID

16 Burnie: 0000-0002-6426-6727

17 Nagahara: 0000-0001-9101-9759

18 Bezodis: 0000-0003-2229-3310

19 **Abstract**

20 In track sprinting, acceleration performance is largely determined by the ability to generate a
21 high ratio of forces (RF), but the technical features associated with this remain unknown. This
22 study therefore investigated the relationships between selected kinematic characteristics and
23 RF during the initial acceleration phase. Fourteen male sprinters completed two maximal 60
24 m sprints from a block start. Full-body kinematic and external kinetic data were obtained from
25 the first four steps, and the relationships between selected kinematic characteristics and mean
26 RF over the first four steps were determined. Placing the stance foot further behind (or less
27 far in front of) the whole-body centre of mass at touchdown was significantly related to greater
28 RF ($r = -0.672$), and more anterior orientation of the proximal end of the foot ($r = -0.724$) and
29 shank ($r = -0.764$) segments at touchdown were also significantly related to greater RF.
30 Following touchdown, greater ankle dorsiflexion range of motion during early stance was
31 significantly related to greater RF ($r = 0.728$). When aiming to enhance RF during initial
32 acceleration, practitioners should be encouraged to focus on lower leg configurations when
33 manipulating touchdown distance, and the role of dorsiflexion during early stance is also an
34 important consideration.

35

36

37 **Keywords**

38 ground reaction forces, performance, sprint start, sprinting, technique, track and field

39

40

41 Word count: 4,394

42 Introduction

43

44 Maximal sprint running is typically broadly divided into acceleration, maximum velocity, and
45 deceleration phases (Volkov & Lapin, 1979; Mero et al., 1992). The first step of a sprint is
46 when the largest forward accelerations are observed, with the magnitude of acceleration
47 progressively decreasing with each successive step (Nagahara et al., 2018a). During this
48 initial acceleration phase, athletes typically reach approximately 70% of their maximum
49 velocity by the end of step four (Nagahara et al., 2014; 2020; 2021). Whilst large ground
50 reaction forces and impulses are required to achieve this acceleration, a key element of high
51 performance during the acceleration phase is the effective orientation of the external force
52 vector (Morin et al., 2011; Rabita et al., 2015; Samozino et al., 2016). This 'technical ability' is
53 typically quantified by the ratio of forces (RF), which describes the proportion of the step-
54 averaged resultant ground reaction force vector (F_R) that is directed horizontally (F_H), i.e., RF
55 $= F_H/F_R$ (Morin et al., 2011).

56

57 Although it has been established that RF is a determining factor for sprint acceleration
58 performance (Kugler and Janshen, 2010; Morin et al., 2011; Rabita et al., 2015), the
59 relationships between stance leg and whole-body kinematics and RF during acceleration
60 remain unknown. Previous investigations have highlighted kinematic characteristics that may
61 be favourable for performance or for the production of horizontal propulsive forces during
62 acceleration (Jacobs & van Ingen Schenau, 1992; Kugler & Janshen, 2010; Bezodis et al.,
63 2015; 2017), but the relationships between these kinematic characteristics and RF were not
64 directly investigated. During the second step of a maximal sprint, Jacobs and van Ingen
65 Schenau (1992) found that highly trained sprinters delayed 'extension' of the whole-body
66 centre of mass (CM) away from the base of support until the CM had been 'rotated' further
67 forwards about the base of support. These findings suggest that changes in the configuration
68 of body segments to assist the forward translation of the whole-body CM during the early part
69 of stance may be favourable for performance.

70
71
72
73
74
75
76
77
78
79
80
81
82
83
84
85
86
87
88
89
90
91
92
93
94
95
96
97

Whilst Jacobs and van Ingen Schenau (1992) reported stance leg joint kinematics and suggested potential kinematic and muscular mechanisms behind the delayed CM 'extension', they did not report relationships to quantify this. Kugler and Janshen (2010) found that greater forward lean of the body throughout stance (defined as the angle between the whole-body CM, centre of pressure, and the global vertical) was associated with a higher RF, and this was facilitated by a more posterior foot placement, whilst Bezodis et al. (2015) used computer simulation to determine that placing the foot further back at touchdown relative to the CM led to a near linear increase in RF during stance. The available research therefore suggests that the stance foot position relative to the CM, often termed touchdown distance when measured at the instant of touchdown, could influence RF.

It is important to consider that the stance leg is multi-segmented, so achieving a position in which the stance foot is further behind a given whole-body CM position at touchdown is primarily a function of the stance ankle, knee, and hip joint angles because the CM position is largely predetermined from the prior toe-off. In previous research, these kinematics were either not reported (Kugler & Janshen, 2010), not related directly to RF (Jacobs and van Ingen Schenau, 1992), or were directly theoretically manipulated (Bezodis et al., 2015). Acute experimental alterations to kinematics during sprint acceleration have been attempted (Bezodis et al., 2017), and it was found that greater antero-posterior force production during stance was preceded by a more dorsiflexed ankle and a more flexed knee at touchdown, and greater hip extension velocity at touchdown. However, Bezodis et al. (2017) used a simple acute experimental within-athlete design with field sports athletes, and further cross-sectional research considering both linear and angular kinematic characteristics in trained sprinters during initial acceleration is required.

There is clearly a need to understand whether certain kinematic features of technique are exhibited by athletes who are capable of achieving higher RF values, and therefore

98 performance levels, during initial acceleration. The aim of this study was therefore to
99 determine the relationships between selected kinematic characteristics and RF during initial
100 acceleration, and consequently to quantify how the kinematic characteristics which are related
101 to RF also relate to overall initial acceleration performance. It was firstly hypothesised that a
102 more negative touchdown distance (i.e. landing with the stance foot further behind/less far in
103 front of the CM) would be associated with a greater ratio of forces during the first four steps of
104 a maximal effort sprint, and that specific joint and segment angular kinematics would underpin
105 this. Secondly, it was also hypothesised that a more negative touchdown distance would be
106 associated with greater initial acceleration performance.

107

108

109 **Methods**

110

111 *Participants*

112 Fourteen collegiate-level male sprinters (mean \pm SD; age: 20 ± 1 years, height: 1.73 ± 0.07
113 m, mass: 68.6 ± 4.9 kg, 100 m personal best time: 11.15 ± 0.33 s [min = 10.68 s; max =
114 11.67 s]) provided written informed consent to participate, and the study was approved by the
115 local research ethics committee. All participants were injury-free and trained five days per
116 week at the time of data collection; they had 8.1 ± 1.8 years of sprint training experience (range
117 = 5 to 10 years). All data were collected over 11 days in early August 2020 during the
118 competition phase of the season (no major COVID-19 training restrictions had been in place
119 since May and domestic competitions were re-started in July).

120

121 *Data collection*

122 Participants completed their preferred self-led warm-up routine. After setting the starting
123 blocks to their preference, two maximal sprint efforts were performed up to 60 m, wearing
124 spiked shoes on an indoor athletics track. Participants were provided with a rest period of at
125 least 10 minutes between sprint efforts. All data were collected from five sessions over 10

126 days, with a temperature and atmospheric pressure (mean \pm SD) of $31.3 \pm 0.9^\circ\text{C}$ and $1010 \pm$
127 2 kPa, respectively.

128

129 Three-dimensional trajectories of 47 retro-reflective markers attached to each participant were
130 captured at 250 Hz using a 16-camera motion capture system (Kestrel 4200, Motion Analysis
131 Corporation, California, USA). The cameras were positioned to capture data up to the end of
132 the fourth step and the markers were placed according to the model of Suzuki et al. (2014).
133 Ground reaction force (GRF) data were collected at 1000 Hz from 52 force plates (TF-3055,
134 TF-32120, TF-90100, Tec Gihan, Uji, Japan) mounted in series under the track. An electric
135 starting gun was used to synchronously initiate GRF data collection, send a pulse to the motion
136 capture system, and emit an auditory starting signal. The global Z-axis was defined as vertical,
137 Y as horizontal in the direction of the running lane, and X as the cross product of the Y- and
138 Z-axes.

139

140 *Data processing*

141 The marker trajectories were exported to Visual3D (v6, C-Motion, Maryland, USA), where they
142 were smoothed using a 4th order low-pass Butterworth filter at a cut-off frequency of 14 Hz,
143 which was selected using residual analysis (Winter, 2009). Kinematic data were resampled at
144 1000 Hz using an interpolating cubic spline to align with the kinetic data. A 15-segment rigid-
145 body model was created, consisting of hands, forearms, upper arms, feet, shanks, thighs,
146 head, upper trunk, and lower trunk (full details are available in Nagahara et al. (2014) and
147 Suzuki et al. (2014)). Each segment was reconstructed from the corresponding markers using
148 a six degrees-of-freedom approach (Spoor & Veldpaus, 1980). The position of the whole-body
149 CM was calculated using the segmental inertia parameters of Japanese athletes (Ae et al.,
150 1992), with 200 g added to each foot to account for the mass of the shoe (Hunter et al., 2004).

151

152 Analysis of the GRF data was conducted using MATLAB (R2021a, Natick, USA). Movement
153 onset was defined as the instant at which the raw vertical GRF signal exceeded, and

154 remained, two standard deviations above the mean signal from the period in which participants
155 were deemed clearly stationary in the blocks (Bezodis et al., 2021). Where participants
156 contacted the track across two adjacent force plates, the required data were reconstructed
157 using the approach outlined by Exell et al. (2012). A 50 N threshold in raw vertical GRF data
158 was used to define contact with the track. Following the identification of touchdown and toe-
159 off using raw signals, each component of the raw GRF data was smoothed using a 4th order
160 low-pass Butterworth filter at a cut-off frequency of 50 Hz (Nagahara et al., 2017; 2018b).

161

162 To calculate instantaneous horizontal velocity (v_H), the net anteroposterior force (i.e., filtered
163 anteroposterior GRF component minus drag force) was divided by body mass and integrated
164 (trapezium rule) with respect to time (Colyer et al., 2018; Samozino et al., 2016). The drag
165 force during each trial was estimated using the athlete's height and mass, and the
166 aerodynamic friction coefficient (Arsac and Locatelli, 2002; Samozino et al., 2016). Horizontal
167 velocity was then integrated (trapezium rule) with respect to time to calculate horizontal CM
168 displacement, which was expressed relative to CM location in the "set" position.

169

170 Contact time and flight time for each of the first four steps were calculated from touchdown
171 and toe-off timings. So that our analysis started from the instant of the first contact on the
172 track, we defined a step as the ground contact phase followed by the subsequent flight phase.
173 Step time was calculated as the sum of contact time and flight time, and step frequency
174 (steps/s) as the inverse of total step time. Step length (m) was determined from the
175 anteroposterior centre of pressure data, where values were extracted from mid-stance. The
176 horizontal and vertical components of displacement and velocity of the whole-body CM were
177 extracted at each touchdown and toe-off.

178

179 Joint angles were calculated for the ankle, knee, and hip joints from the respective adjacent
180 segments using Cardan/Euler angles (Robertson et al., 2004), with extension/plantar flexion
181 defined as positive (Figure 1a). Ankle angle was defined as the angle between the shank and

182 rearfoot segments, with the latter defined from the ankle to the metatarsophalangeal (MTP)
183 joint centres. Angular velocities for each joint were expressed as the distal segment relative
184 to the proximal segment, using the proximal segment as the resolution coordinate system
185 (Bezodis et al., 2017). Absolute segment angles were also calculated for the foot, shank, thigh,
186 and (upper) trunk. These were expressed relative to the horizontal with positive rotation
187 representing an anti-clockwise rotation of the proximal end about the distal end when viewed
188 from the right hand side (Figure 1b). For these absolute segment angles, the foot was
189 modelled as a single rigid segment from the toe marker to the heel marker to provide a general
190 representation of the orientation of the foot as a whole.

191

192 **** Figure 1 near here ****

193

194 Foot touchdown velocity was defined as the global Y-axis component of the distal endpoint
195 velocity of the foot at each touchdown. The global Y-axis displacement between each toe
196 marker and the whole-body CM was calculated, and the value of this for the stance foot at
197 each touchdown and toe-off were extracted as touchdown distance and toe-off distance,
198 respectively, with a negative value representing the foot behind the CM. Touchdown and toe-
199 off distances, CM height and step length were normalised to account for differences in leg
200 length between sprinters by dividing each by the individual's greater trochanter height.
201 Discrete angular kinematics (e.g., angles and angular velocities at touchdown and toe-off,
202 peak and minimum values, ranges of motion (RoM)) were extracted from the continuous
203 angular kinematic waveforms (see Figure 2 for definitions).

204

205 **** Figure 2 near here ****

206

207 Step-averaged kinetic data from each of the first four stance phases were determined from
208 the resultant GRF (F_R) and its vertical (F_V) and antero-posterior (F_H) components. Step-
209 averaged RF was then calculated as step-averaged F_H divided by step-averaged F_R (Bezodis

210 et al., 2021). RF over each of the first four steps was averaged (RF_{MEAN}) and used as the
211 dependent measure against which to correlate the kinematic characteristics. This was
212 selected based on the prior work of King et al. (2021) who identified that step-to-step variation
213 in RF (and linearity in the RF- v_H profile) was not related to initial acceleration performance;
214 RF_{MEAN} over the first four steps was identified as the metric derived from the RF- v_H relationship
215 most strongly related to performance during the initial acceleration phase.

216

217 Average horizontal external power from the beginning of the first contact to the end of the
218 fourth contact was calculated as the change in external kinetic energy of the CM (based on
219 horizontal CM velocity) divided by the change in time over this period (Bezodis et al., 2010).
220 These external power data were normalised to dimensionless values to account for differences
221 in stature (Bezodis et al., 2010; Hof, 1996). Normalised average horizontal external power
222 (NAHEP) over these four steps was used as an objective measure of initial acceleration phase
223 performance.

224

225 *Statistical analysis*

226 Consistent with similar sprint acceleration biomechanics research which has related features
227 of technique to performance (e.g. Nagahara et al., 2017; 2018a), the trial with the highest
228 performance was analysed. The trial in which each participant displayed the highest NAHEP
229 was therefore used in all statistical analyses (for three of the sprinters only one trial was
230 available due to incomplete data), which were conducted in SPSS (v28.0, IBM, Illinois, USA).
231 Bivariate correlations (Pearson's r) between the four-step mean value of each of the kinematic
232 variables of interest (Tables 1-3) and RF_{MEAN} were performed, with statistical significance
233 accepted at $p < 0.05$. Following this, the bivariate correlations with NAHEP for each of the
234 variables which were significantly related to RF_{MEAN} were determined. Thresholds for the
235 magnitudes of all correlation coefficients were defined according to Batterham and Hopkins
236 (2006) as trivial (0.0), small (0.1), moderate (0.3), large (0.5), very large (0.7), nearly perfect

237 (0.9) and perfect (1.0). Descriptive statistics are presented as mean values (\pm SD) across the
238 14 sprinters.

239

240

241 **Results**

242

243 *Relationships between linear kinematics, spatiotemporal variables, and RF*

244 The correlation coefficient between RF_{MEAN} and normalised touchdown distance over the four
245 steps was large and significant ($r = -0.672$, $p < 0.01$; Table 1; Figure 3a), with its negative
246 direction indicating that touchdown foot placement further behind the CM (or less far in front
247 of the CM as the acceleration phase progressed) was associated with higher RF. A very large,
248 significant correlation coefficient was found between mean step frequency and RF_{MEAN} ($r =$
249 0.715 , $p < 0.01$; Figure 3b). The correlation coefficients between RF_{MEAN} and all other linear
250 kinematics ranged from trivial to moderate and were not significant (Table 1).

251

252 **** Table 1 near here ****

253 ****Figure 3 near here****

254

255 *Relationships between angular kinematics and RF*

256 There was a very large significant correlation coefficient between mean ankle dorsiflexion RoM
257 and RF_{MEAN} ($r = 0.728$ $p < 0.01$; Figure 3c) during the initial acceleration phase (Table 2). All other
258 correlation coefficients between RF_{MEAN} and the ankle, knee, and hip joint angular kinematics
259 ranged from trivial to moderate and were not significant (Table 2).

260

261 Very large, significant correlation coefficients were observed between both mean foot and
262 shank angle at touchdown and RF_{MEAN} ($r = -0.724$ and -0.764 , respectively, both $p < 0.01$;
263 Table 3; Figures 3d and 3e). As these coefficients were negative, they relate to higher RF_{MEAN}
264 being associated with more forward-orientated proximal ends of the foot and shank segments

265 (see Figure 1b). There were no other significant correlation coefficients between RF_{MEAN} and
266 the remaining segment angular kinematic variables, although the coefficient with mean shank
267 angle at toe-off was large ($r = -0.511$, $p = 0.06$; Table 3).

268

269 ****Table 2 near here****

270 **** Table 3 near here ****

271

272 *Relationships between kinematics favourable for RF and initial acceleration phase*
273 *performance*

274 Of the kinematic characteristics that were significantly related to RF_{MEAN} , only mean normalised
275 touchdown distance was also significantly related to NAHEP over the four steps ($r = -0.710$,
276 $p < 0.01$; Figure 3f). Moderate correlation coefficients with initial acceleration performance were
277 found for each of the other measures related to RF_{MEAN} (Table 4), and all were in the same direction
278 as the relationships between the respective variables and RF_{MEAN} .

279

280 **** Table 4 near here ****

281

282

283 **Discussion**

284 This study determined the relationships between selected kinematic characteristics and RF
285 during the initial acceleration phase of sprinting, and quantified how those which were related
286 to RF also related to overall initial acceleration performance. Our first hypothesis was accepted
287 as landing with the stance foot further behind/less far in front of the CM (i.e., a more negative
288 touchdown distance) was associated with better 'technical ability' during initial acceleration,
289 namely a significantly greater RF_{MEAN} over the first four steps, and a higher step frequency
290 was also associated with a greater RF_{MEAN} . Specific angular kinematics underpinned this; a
291 more forwards orientated foot and shank at touchdown, as well as greater ankle dorsiflexion
292 range of motion during early stance, were associated with significantly greater RF_{MEAN} . Of

293 these kinematic characteristics associated with RF_{MEAN} , only normalised touchdown distance
294 was also significantly related to performance (NAHEP) over the initial acceleration phase, and
295 thus our second hypothesis was also accepted.

296

297 The very large negative correlation coefficient between touchdown distance and RF_{MEAN} over
298 the initial acceleration phase is a novel finding which extends the current understanding.
299 Jacobs and van Ingen Schenau (1992) had previously identified the need for the CM to be
300 'rotated' further ahead of the stance foot before it is 'extended' away from it, and Kugler and
301 Janshen (2010) had identified a link between touchdown distance and propulsive force
302 magnitude. The current findings extend this to RF and raise the possibility that a more negative
303 touchdown distance could be one means through which to reduce the requirement for 'rotation'
304 of the CM prior to it 'extending' away from the stance foot. The current study also extends from
305 the findings of Bezodis et al. (2017) by directly identifying this relationship between touchdown
306 distance and RF in a cohort of well-trained sprinters. Although it is not possible to keep the
307 stance foot behind the whole-body CM at touchdown throughout the initial acceleration phase
308 (mean touchdown distance progressively increased from steps 1 to 4, respectively: -0.15,
309 -0.05, 0.02, 0.07 [normalised to greater trochanter height]), aiming to limit the increase in
310 touchdown distance by keeping the stance foot as close to the whole-body CM as possible
311 once touchdown distances become positive appears preferable.

312

313 For a given CM position at touchdown, which is largely determined from the prior instant of
314 toe-off given the projectile motion of the sprinter's CM during flight, touchdown distance must
315 primarily be manipulated through kinematics of the leg swinging through to become the stance
316 leg at touchdown. More forwards rotated proximal ends (see Figure 1b) of the foot and shank
317 segments at touchdown over the first four steps were also associated with achieving a high
318 RF_{MEAN} during initial acceleration (Table 3). The very large relationships confirm the
319 importance of these lower leg segment orientations for high RF production during initial
320 acceleration and identify potential specific kinematic features which may be important for

321 achieving a high RF through a more negative touchdown distance. Although Bezodis et al.
322 (2017) experimentally manipulated technique and only reported angles about joints, the
323 current cross-sectional results appear to align with their within-individual results given the
324 importance of the lower part of the leg. As ankle angle at touchdown was not significantly
325 related to RF_{MEAN} in the current study, sprinters who achieved a higher RF during initial
326 acceleration did not typically have a more plantarflexed or dorsiflexed ankle at touchdown.
327 Given the linked-segment nature of the swinging leg prior to touchdown, this suggests that the
328 more forward orientation of the foot and shank was likely primarily achieved through a change
329 in shank orientation. This supports the applied interest in shin (i.e., shank) angles (von Lieres
330 und Wilkau et al., 2020), but practitioners should therefore also be cognisant of the orientation
331 of the foot to ensure that a more forward shank orientation is also accompanied by a more
332 forward foot orientation, and that any attempts to manipulate shank angle do not negatively
333 affect the foot and ankle kinematics.

334

335 Immediately after touchdown, the ankle dorsiflexed for a short period during the early part of
336 each stance phase (mean ankle dorsiflexion RoM was 13°, 13°, 15°, 16° in steps 1 to 4,
337 respectively). The very large positive relationship between the average dorsiflexion RoM and
338 RF_{MEAN} over four steps is novel and provides further empirical support for the theory of Jacobs
339 and van Ingen Schenau (1992). These findings suggest that ankle dorsiflexion may be a
340 primary means through which the CM can be 'rotated' forwards about the foot during early
341 stance before the sequential proximal-to-distal extension of the stance leg joints (Jacobs &
342 van Ingen Schenau, 1992; Charalambous et al., 2012; Bezodis et al., 2014; Brazil et al., 2017;
343 Bezodis et al., 2019) then 'extends' the CM away from the foot as the stance phase
344 progresses. This provides evidence for a specific mechanism through which the more general
345 'rotate' then 'extend' strategy of Jacobs and van Ingen Schenau (1992) could be realised when
346 considering the action of the linked segments within the system. This finding also provides
347 empirical support for the 'shin roll' conceptual framework of Alt et al. (2022) which proposes
348 the need for the shank to rotate forwards about a relatively stationary foot segment. Whilst the

349 current findings provide new evidence to potentially support this theory, and to confirm a
350 relationship between ankle dorsiflexion and the ability to generate a higher RF, quantification
351 of the coordination of shank and foot motion is required to provide a more complete
352 understanding of the complex role of the foot, ankle and shank during early stance in sprint
353 acceleration (Donaldson et al., 2022). However, it must also be considered that ankle
354 dorsiflexion may be constrained by a sprinter's passive range of motion. Further direct
355 investigation with more complex foot models where possible, as well as consideration of the
356 coordination between segments, is required to better understand foot-ankle-shank motion
357 during early acceleration. Furthermore, given that limiting dorsiflexion during early stance
358 when in a more upright configuration in maximal velocity sprinting may be important for
359 performance (Nagahara and Zushi, 2017), consideration should also be given to the changing
360 demands of different sprint phases.

361

362 The very large positive correlation coefficient between average step frequency and RF_{MEAN} during
363 initial acceleration is likely a function of a relatively smaller vertical impulse component being
364 applied. As a large relative horizontal component of F_R is fundamentally required for achieving
365 high RF, this is inherently accompanied by a relatively smaller vertical component of the
366 vector. As F_R and RF were not related in the current study ($r = -0.176$), this suggests that
367 higher step frequencies may be a function of the RF achieved (i.e., the relatively smaller
368 vertical component of the GRF did not prolong contact time and led to higher step
369 frequencies), rather than being a technical feature that leads to a higher RF. However, due to
370 the nature of the study design, causality cannot be determined and the interaction between
371 RF and step frequency during initial acceleration may warrant further direct investigation.

372

373 Having identified kinematic features which were related to RF during initial acceleration, it was
374 important to also consider the role of these in overall performance, or to identify any potentially
375 conflicting findings between RF-associated kinematics and performance-associated
376 kinematics. Of the RF-associated kinematics, only average normalised touchdown distance

377 was also significantly related to performance over the initial acceleration phase. Each of the
378 other kinematic characteristics of interest were moderately, but non-significantly, related to
379 performance. Whilst some caution must therefore be given to ensure that any technical
380 changes intended to affect RF actually translate to performance improvements, the fact that
381 each of the relationships observed with performance were in the same direction as those
382 observed with RF_{MEAN} , give confidence that they are unlikely to be detrimental to performance
383 for a given individual. However, further investigation is required to understand the additional
384 technical or physical features which may be required in order to translate a change in a given
385 kinematic variable and in RF, to a change in performance. As an example, Bezodis et al.
386 (2015) demonstrated through computer simulation that progressively more negative
387 touchdown distances (achieved through manipulations to knee joint angle) were associated
388 with greater RF, but the ability for this to continue contributing to increased performance was
389 limited because touchdown distances which became too negative limited the ability of the
390 sprinter to produce the necessary vertical impulse.

391

392 Whilst the current study provides new empirical data to support existing theories, it is not without
393 limitations. Due to the applied nature of the data collection undertaken only a simple model of the
394 foot was used. Whilst different foot models were used to quantify each of the ankle and foot motion
395 separately, future studies which are able to implement more complex foot models would be ideal
396 given the clear importance of the foot-ankle-shank complex, but these are challenging to implement
397 with sufficient internal and ecological validity in a sprint environment. Furthermore, we only
398 considered the joint and segment kinematics; the underlying joint kinetics were not investigated. It
399 may be useful for future studies to consider the joint moment and power profiles at the ankle,
400 particularly during the energy absorption phase in early stance when the ankle is dorsiflexing
401 (Bezodis et al., 2014), and also to consider the MTP joint kinetics if more complex foot models can
402 be implemented (Bezodis et al., 2012). Future work could also consider analysis of the swing leg
403 kinematics to understand its potential role in the CM kinematics and RF, the potential role of
404 movements outside of the sagittal plane, and how sprinters coordinate their movements to obtain

405 the specific body configurations identified at touchdown in the current study. Our analysis also
406 removed the block phase from consideration so that block phase performance did not bias our
407 direct comparison of technique and performance during the first four steps on the track as block
408 phase RF values do not always correspond well with the subsequent steps (e.g. Bezodis et al.,
409 2021; Rabita et al., 2015). Future research may also wish to consider, or account for, the influence
410 of block phase performance, for example using the approach adopted by King et al. (2021).

411

412 During the initial acceleration phase, placement of the stance foot in a more posterior position
413 relative to the CM at touchdown is significantly associated with a higher mean RF. A more
414 forward orientation of both the foot and shank segments at touchdown was also associated
415 with higher RF and thus practitioners should pay particular attention to the orientation of the
416 lower stance leg when focussing on touchdown distance manipulations. Immediately after
417 touchdown, a greater ankle dorsiflexion range of motion is also significantly associated with a
418 higher mean RF, and these empirical data have revealed specific linear and angular kinematic
419 features of technique which provide further detail to underpin existing sprint acceleration
420 theories.

421

422

423 **Acknowledgements**

424 The authors are grateful to Dr Sam Gleadhill (University of South Australia, Australia) for his
425 assistance during data collection. There was no financial assistance with this project.

426

427

428 **Conflict of interest statement**

429 The authors report there are no competing interests to declare.

430

431

432

433 **References**

434 Ae, M., Tang, H. and Yokoi, T. (1992). Estimation of inertia properties of the body segments
435 in Japanese athletes. *Biomechanisms*, 11, 23-33. Doi: [10.3951/biomechanisms.11.23](https://doi.org/10.3951/biomechanisms.11.23).

436

437 Alt, T., Oeppert, T. J., Zedler, M., Goldmann, J.-P., Braunstein, B. and Willwacher, S. (2022).

438 A novel guideline for the analysis of linear acceleration mechanics – outlining a conceptual

439 framework of ‘shin roll’ motion. *Sports Biomechanics*, in press. Doi:

440 [10.1080/14763141.2022.2094827](https://doi.org/10.1080/14763141.2022.2094827).

441

442 Arsac, L.M. and Locatelli, E. (2002). Modeling the energetics of 100-m running by using

443 speed curves of world champions. *Journal of Applied Physiology*, 92(5), 1781-1788. Doi:

444 [10.1152/jappphysiol.00754.2001](https://doi.org/10.1152/jappphysiol.00754.2001).

445

446 Batterham, A. and Hopkins, W. (2006). Making meaningful inferences about magnitudes.

447 *International Journal of Sports Physiology and Performance*, 1, 50-57.

448 Doi: [10.1123/ijsp.1.1.50](https://doi.org/10.1123/ijsp.1.1.50).

449

450 Bezodis, N.E., Colyer, S., Nagahara, R., Bayne, H., Bezodis, I.N., Morin, J.-B., Murata, M.

451 and Samozino, P. (2021). Ratio of forces during sprint acceleration: A comparison of

452 different calculation methods. *Journal of Biomechanics*, 127(5), 110685.

453 Doi: [10.1016/j.jbiomech.2021.110685](https://doi.org/10.1016/j.jbiomech.2021.110685).

454

455 Bezodis, N.E., North, J.S. and Razavet, J.L. (2017). Alterations to the orientation of the

456 ground reaction force vector affect sprint acceleration performance in team sports athletes.

457 *Journal of Sports Sciences*, 35(18), 1817-1824. Doi: [10.1080/02640414.2016.1239024](https://doi.org/10.1080/02640414.2016.1239024).

458

459 Bezodis, N.E., Salo, A.I.T. and Trewartha, G. (2010). Choice of sprint start performance

460 measure affects the performance-based ranking within a group of sprinters: which is the

461 most appropriate measure? *Sports Biomechanics*, 9(4), 258-269.

462 Doi: [10.1080/14763141.2010.538713](https://doi.org/10.1080/14763141.2010.538713).

463

464 Bezodis, N. E., Salo, A. I. T. and Trewartha, G. (2012). Modeling the stance leg in two-
465 dimensional analyses of sprinting: inclusion of the MTP joint affects joint kinetics. *Journal of*
466 *Applied Biomechanics*, 28, 222-227. Doi: [10.1123/jab.28.2.222](https://doi.org/10.1123/jab.28.2.222).

467

468 Bezodis, N. E., Salo, A. I. T. and Trewartha, G. (2014). Lower limb joint kinetics during the first
469 stance phase in athletics sprinting: three elite case-studies. *Journal of Sports Sciences*, 32,
470 738-746. Doi: [10.1080/02640414.2013.849000](https://doi.org/10.1080/02640414.2013.849000).

471

472 Bezodis, N.E., Trewartha, G. and Salo, A.I.T. (2015). Understanding the effect of touchdown
473 distance and ankle joint kinematics on sprint acceleration performance through computer
474 simulation. *Sports Biomechanics*, 14(2), 232-245. Doi: [10.1080/14763141.2015.1052748](https://doi.org/10.1080/14763141.2015.1052748).

475

476 Bezodis, N. E., Willwacher, S. and Salo, A. I. T. (2019). The biomechanics of the track and
477 field sprint start: a narrative review. *Sports Medicine*, 49(9), 1345-1364. Doi:
478 [10.1007/s40279-019-01138-1](https://doi.org/10.1007/s40279-019-01138-1).

479

480 Brazil, A., Exell, T., Wilson, C., Willwacher, S., Bezodis, I. and Irwin, G. (2017). Lower limb
481 joint kinetics in the starting blocks and first stance in athletic sprinting. *Journal of Sports*
482 *Sciences*, 35(16), 1629-1635. Doi: [10.1080/02640414.2016.1227465](https://doi.org/10.1080/02640414.2016.1227465)

483

484 Charalambous, L., Irwin, G., Bezodis, I. N. and Kerwin, D. (2012). Lower limb joint kinetics
485 and ankle joint stiffness in the sprint start push-off. *Journal of Sports Sciences*, 30(1), 1-9.
486 Doi: [10.1080/02640414.2011.616948](https://doi.org/10.1080/02640414.2011.616948)

487

488 Colyer, S. L., Nagahara, R. and Salo, A. I. T. (2018). Kinetic demands of sprinting shift
489 across the acceleration phase: novel analysis of entire force waveforms. *Scandinavian*
490 *Journal of Medicine and Science in Sports*, 28(7), 1784-1792. Doi: [10.1111/sms.13093](https://doi.org/10.1111/sms.13093).
491

492 Donaldson, B. J., Bayne, H. and Bezodis, N. E. (2022). Inter- and intra-limb coordination
493 during initial sprint acceleration. *Biology Open*, 11, bio059501. Doi: [10.1242/bio.059501](https://doi.org/10.1242/bio.059501).
494

495 Exell, T. A., Gittoes, M. J. R., Irwin, G. & Kerwin, D. G. (2012). Considerations of force plate
496 transitions on centre of pressure calculation for maximal velocity sprint running. *Sports*
497 *Biomechanics*, 11(4), 532-541. Doi: [10.1080/14763141.2012.684698](https://doi.org/10.1080/14763141.2012.684698)
498

499 Hof, A. (1996). Scaling gait data to body size. *Gait & Posture*, 4, 222-223. Doi:
500 [10.1016/0966-6362\(95\)01057-2](https://doi.org/10.1016/0966-6362(95)01057-2).
501

502 Hunter, J., Marshall, R. and McNair, P. (2004). Interaction of step length and step rate during
503 sprint running. *Medicine & Science in Sports & Exercise*, 36(2), 261-271. Doi:
504 [10.1249/01.MSS.0000113664.15777.53](https://doi.org/10.1249/01.MSS.0000113664.15777.53).
505

506 Jacobs, R. and van Ingen Schenau, G. J. (1992). Intermuscular coordination in a sprint
507 push-off. *Journal of Biomechanics*, 25(9), 953-965. Doi: [10.1016/0021-9290\(92\)90031-u](https://doi.org/10.1016/0021-9290(92)90031-u).
508

509 King, D., Burnie, L., Nagahara, R. and Bezodis, N. (2021). Linearity of the ratio of forces-
510 velocity relationship is not related to initial acceleration performance in sprinting.
511 *Proceedings of the XXXIX Annual Conference of the International Society of Biomechanics*
512 *in Sports*, 39, 292-295.
513

514 Kugler, F. and Janshen, L. (2010). Body position determines propulsive forces in accelerated
515 running. *Journal of Biomechanics*, 43, 343-348. Doi: [10.1016/j.jbiomech.2009.07.041](https://doi.org/10.1016/j.jbiomech.2009.07.041).

516

517 Mero, A., Komi, P. V. & Gregor, R. J. (1992). Biomechanics of sprint running: a review. *Sports*
518 *Medicine*, 13(6), 376-392. Doi: [10.2165/00007256-199213060-00002](https://doi.org/10.2165/00007256-199213060-00002).

519

520 Morin, J.-B., Edouard, P. and Samozino, P. (2011). Technical ability of force application as a
521 determinant factor of sprint performance. *Medicine and Science in Sports and Exercise*,
522 43(9), 1680-1688. Doi: [10.1249/MSS.0b013e318216ea37](https://doi.org/10.1249/MSS.0b013e318216ea37).

523

524 Nagahara, R., Kanehisa, H. and Fukunaga, T. (2020). Ground reaction force across the
525 transition during sprint acceleration. *Scandinavian Journal of Medicine & Science in Sports*,
526 30(3), 450-461. Doi: [10.1111/sms.13596](https://doi.org/10.1111/sms.13596).

527

528 Nagahara, R., Kanehisa, H., Matsuo, A. and Fukunaga, T. (2021). Are peak ground reaction
529 forces related to better sprint acceleration performance? *Sports Biomechanics*, 20(3), 363-
530 369. Doi: [10.1080/14763141.2018.1560494](https://doi.org/10.1080/14763141.2018.1560494).

531

532 Nagahara, R., Matsubayashi, T., Matsuo, A. and Zushi, K. (2014). Kinematics of transition
533 during human accelerated sprinting. *Biology Open*, 3(8), 689-699. Doi:
534 [10.1242/bio.20148284](https://doi.org/10.1242/bio.20148284).

535

536 Nagahara, R., Mizutani, M., Matsuo, A., Kanehisa, H. and Fukunaga, T. (2017). Association
537 of step width with accelerated sprinting performance and ground reaction force. *International*
538 *Journal of Sports Medicine*, 38, 534-540. Doi: [10.1055/s-0043-106191](https://doi.org/10.1055/s-0043-106191)

539

540 Nagahara, R., Mizutani, M., Matsuo, A., Kanehisa, H. and Fukunaga, T. (2018a). Association
541 of sprint performance with ground reaction forces during acceleration and maximal speed
542 phases in a single sprint. *Journal of Applied Biomechanics*, 34(2), 104-110. Doi:
543 [10.1123/jab.2016-0356](https://doi.org/10.1123/jab.2016-0356)

544

545 Nagahara, R., Mizutani, M., Matsuo, A., Kanehisa, H. and Fukunaga, T. (2018b). Step-to-
546 step spatiotemporal variables and ground reaction forces of intra-individual fastest sprinting
547 in a single session. *Journal of Sports Sciences*, 36(12), 1392-1401. Doi:
548 [10.1080/02640414.2017.1389101](https://doi.org/10.1080/02640414.2017.1389101)

549

550 Nagahara, R. and Zushi, K. (2017). Development of maximal speed sprinting performance
551 with changes in vertical, leg and joint stiffness. *The Journal of Sports Medicine and Physical*
552 *Fitness*, 57(12), 1572-1578. Doi: [10.23736/S0022-4707.16.06622-6](https://doi.org/10.23736/S0022-4707.16.06622-6)

553

554 Rabita, G., Dorel, S., Slawinski, J., Sàez-de-Villarreal, E., Couturier, A., Samozino, P. and
555 Morin, J.-B. (2015). Sprint mechanics in world-class athletes: a new insight into the limits of
556 human locomotion. *Scandinavian Journal of Medicine & Science in Sports*, 25(5), 583-594.
557 Doi: [10.1111/sms.12389](https://doi.org/10.1111/sms.12389).

558

559 Robertson, D. G. E., Caldwell, G. E., Hamill, J., Kamen, G. & Whittlesey, S. N. (2004).
560 *Research methods in biomechanics*. Champaign, IL: Human Kinetics.

561

562 Samozino, P., Rabita, G., Dorel, S., Slawinski, J., Peyrot, N., de Villarreal, E. S. and Morin,
563 J.-B. (2016). A simple method for measuring power, force, velocity properties, and
564 mechanical effectiveness in sprint running. *Scandinavian Journal of Medicine & Science in*
565 *Sports*, 26(6), 648-658. Doi: [10.1111/sms.12490](https://doi.org/10.1111/sms.12490).

566

567 Spoor, C. W. and Veldpaus, F. E. (1980). Rigid body motion calculated from spatial co-
568 ordinates of markers. *Journal of Biomechanics*, 13(4), 391-393. Doi: [10.1016/0021-](https://doi.org/10.1016/0021-)

569 [9290\(80\)90020-2](https://doi.org/10.1016/0021-9290(80)90020-2)

570

571 Suzuki, Y., Ae, M., Takenaka, S. and Fujii, N. (2014). Comparison of support leg kinetics
572 between side-step and cross-step cutting techniques. *Sports Biomechanics*, 13(2), 144-153.
573 Doi: [10.1080/14763141.2014.910264](https://doi.org/10.1080/14763141.2014.910264).
574
575 Volkov, N. I. and Lapin, V. I. (1979). Analysis of the velocity curve in sprint running. *Medicine*
576 *and Science in Sports*, 11(4), 332-337.
577
578 von Lieres und Wilkau, H. C., Irwin, G., Bezodis, N. E., Simpson, S. and Bezodis, I. N.
579 (2020). Phase analysis in maximal sprinting: an investigation of step-to-step technical
580 changes between the initial acceleration, transition and maximal velocity phases. *Sports*
581 *Biomechanics*, 19(2), 141-156. Doi: [10.1080/14763141.2018.1473479](https://doi.org/10.1080/14763141.2018.1473479).
582
583 Winter, D. (2009). *Biomechanics and motor control of human movement* (4th ed.). New York,
584 NY: Wiley.

585 List of Tables

586

587 **Table 1.** Mean \pm SD linear kinematics and spatiotemporal variables over the first four steps

588 and their relationships with RF_{MEAN} , including 95% confidence intervals for the r values.

	Four step mean	Correlation (r)	95% Confidence Intervals
Centre of mass			
Normalised CM height at touchdown	0.86 \pm 0.03	0.000	-0.531 : 0.530
Normalised CM height at toe-off	0.95 \pm 0.04	-0.046	-0.563 : 0.497
Normalised touchdown distance	-0.03 \pm 0.04	-0.672**	-0.887 : -0.220
Normalised toe-off distance	-0.89 \pm 0.04	-0.428	-0.781 : 0.132
Spatiotemporal			
Contact time (s)	0.189 \pm 0.014	-0.406	-0.771 : 0.159
Flight time^ (s)	0.078 \pm 0.017	-0.242	-0.685 : 0.331
Normalised step length	1.44 \pm 0.11	-0.296	-0.714 : 0.279
Step frequency (steps/s)	4.26 \pm 0.29	0.715**	0.297 : 0.903
Foot			
Touchdown velocity (m/s)	0.32 \pm 0.44	-0.398	-0.767 : 0.168

589 ^Following contact phase. ** Correlation is significant at the 0.01 level (2-tailed).

590 **Table 2.** Mean \pm SD joint angular kinematics over the first four steps and their relationships
 591 with RF_{MEAN}, including 95% confidence intervals for the r values.

	Four step mean	Correlation (r)	95% Confidence Intervals
Ankle			
<u>Angle^a</u>			
Touchdown (°)	102 \pm 5	0.154	-0.410 : 0.633
Dorsiflexion RoM (°)	14 \pm 3	0.728**	0.321 : 0.908
Peak dorsiflexion (°)	88 \pm 4	-0.258	-0.693 : 0.316
Plantar flexion RoM (°)	53 \pm 3	0.110	-0.447 : 0.605
Toe-off (°)	140 \pm 5	-0.141	-0.625 : 0.421
<u>Angular velocity</u>			
Touchdown (°/s)	-271 \pm 66	-0.072	-0.580 : 0.477
Peak dorsiflexion (°/s)	-457 \pm 56	-0.449	-0.791 : 0.107
Peak plantar flexion (°/s)	1147 \pm 84	0.311	-0.263 : 0.722
Toe-off (°/s)	815 \pm 118	-0.087	-0.590 : 0.465
Knee			
<u>Angle</u>			
Touchdown (°)	117 \pm 5	-0.326	-0.730 : 0.247
Early flexion RoM (°)	0 \pm 1	-0.292	-0.712 : 0.283
Peak flexion (°)	116 \pm 5	-0.277	-0.704 : 0.297
Extension RoM (°)	41 \pm 5	0.149	-0.414 : 0.630
Peak extension (°)	158 \pm 5	-0.168	-0.642 : 0.398
Late flexion RoM (°)	0 \pm 1	0.372	-0.198 : 0.754
Toe-off (°)	158 \pm 5	-0.202	-0.662 : 0.368
<u>Angular velocity</u>			
Touchdown (°/s)	216 \pm 70	-0.226	-0.676 : 0.346
Peak extension (°/s)	636 \pm 89	-0.167	-0.641 : 0.399
Peak flexion (°/s)	-100 \pm 83	-0.228	-0.677 : 0.344
Toe-off (°/s)	-27 \pm 144	-0.413	-0.774 : 0.151
Hip			
<u>Angle</u>			
Touchdown (°)	114 \pm 6	0.295	-0.280 : 0.714
Extension RoM (°)	59 \pm 5	-0.234	-0.680 : 0.339
Toe-off (°)	173 \pm 6	0.098	-0.456 : 0.598
<u>Angular velocity</u>			
Touchdown (°/s)	549 \pm 37	0.201	-0.369 : 0.661
Peak extension (°/s)	604 \pm 32	-0.268	-0.699 : 0.306
Toe-off (°/s)	116 \pm 88	0.036	-0.504 : 0.556

592 ** Correlation is significant at the 0.01 level (2-tailed).

593 **Table 3.** Mean \pm SD segment angular kinematics over the first four steps and their
 594 relationships with RF_{MEAN} , including 95% confidence intervals for the r values.

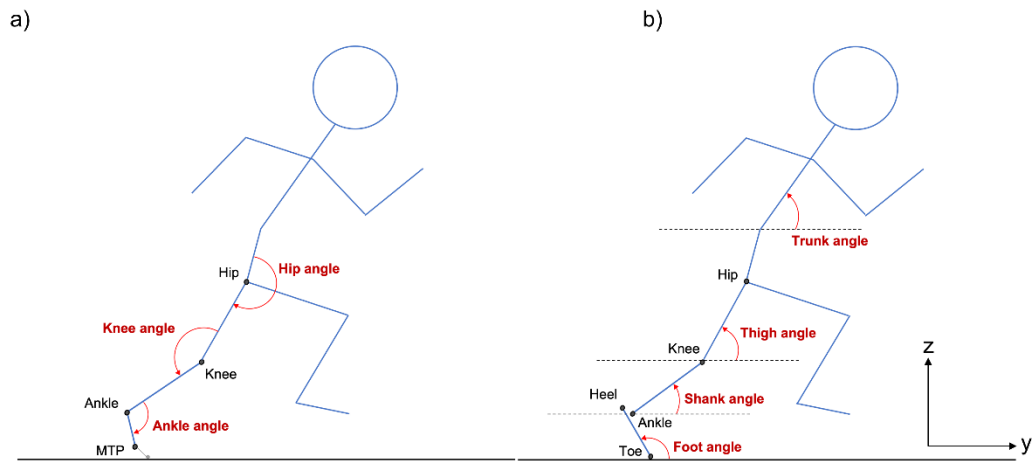
	Four step mean	Correlation (r)	95% Confidence Intervals
Foot			
<u>Angle</u>			
Touchdown ($^{\circ}$)	164 \pm 5	-0.724**	-0.906 : -0.313
Toe-off ($^{\circ}$)	105 \pm 4	-0.334	-0.734 : 0.239
<u>Angular velocity</u>			
Touchdown ($^{\circ}/s$)	-25 \pm 66	0.408	-0.156 : 0.772
Toe-off ($^{\circ}/s$)	-1310 \pm 121	0.214	-0.357 : 0.669
Shank			
<u>Angle</u>			
Touchdown ($^{\circ}$)	55 \pm 3	-0.764**	-0.921 : -0.392
Toe-off ($^{\circ}$)	33 \pm 3	-0.235	-0.680 : 0.338
<u>Angular velocity</u>			
Touchdown ($^{\circ}/s$)	-235 \pm 69	-0.309	-0.721 : 0.265
Toe-off ($^{\circ}/s$)	-142 \pm 65	-0.511	-0.820 : 0.026
Thigh			
<u>Angle</u>			
Touchdown ($^{\circ}$)	118 \pm 3	-0.252	-0.690 : 0.322
Toe-off ($^{\circ}$)	55 \pm 4	0.076	-0.473 : 0.583
<u>Angular velocity</u>			
Touchdown ($^{\circ}/s$)	-456 \pm 32	-0.174	-0.645 : 0.393
Toe-off ($^{\circ}/s$)	-126 \pm 96	0.304	-0.270 : 0.719
Trunk			
<u>Angle</u>			
Touchdown ($^{\circ}$)	34 \pm 8	-0.151	-0.631 : 0.413
Toe-off ($^{\circ}$)	44 \pm 8	-0.180	-0.649 : 0.388
<u>Angular velocity</u>			
Touchdown ($^{\circ}/s$)	-14 \pm 48	-0.272	-0.702 : 0.302
Toe-off ($^{\circ}/s$)	-24 \pm 55	-0.223	-0.674 : 0.348

595 ** Correlation is significant at the 0.01 level (2-tailed).

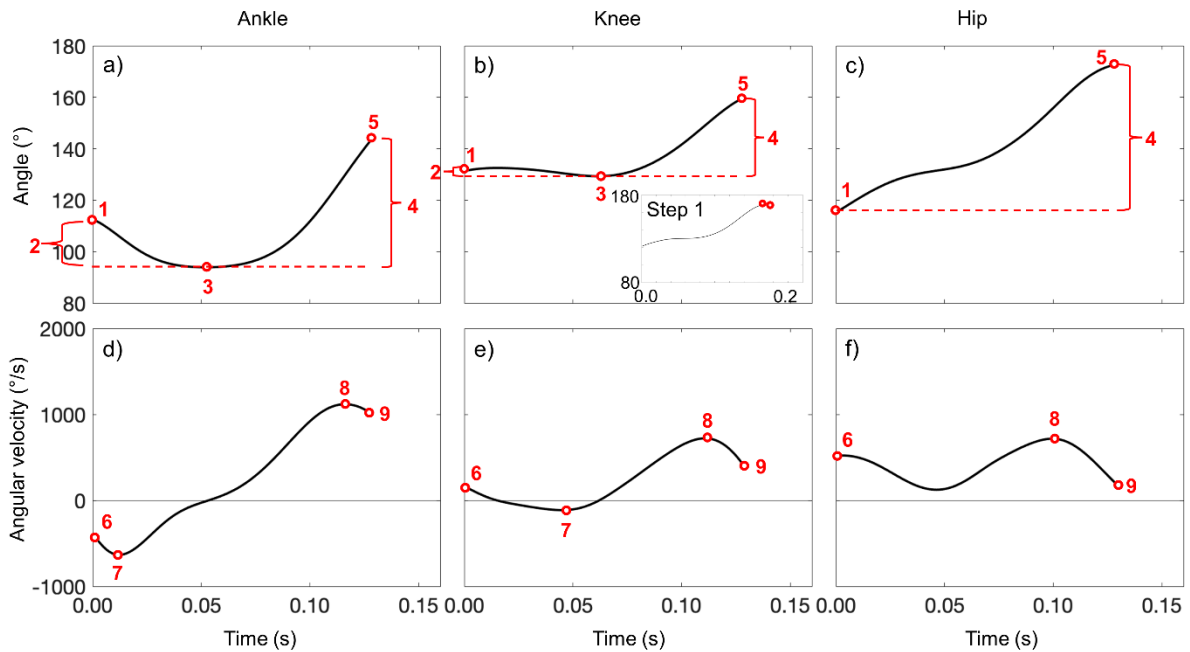
596 **Table 4.** Mean \pm SD relationships between kinematic characteristics favourable for RF_{MEAN}
 597 and their relationships with initial acceleration phase performance (normalised average
 598 horizontal external power; NAHEP), including 95% confidence intervals for the r values.

Measure	Correlation (r)	95% Confidence Intervals
Normalised touchdown distance	-0.710**	-0.901 : -0.287
Step frequency (steps.s ⁻¹)	0.434	-0.126 : 0.784
Ankle dorsiflexion RoM (°)	0.458	-0.096 : 0.795
Touchdown foot angle (°)	-0.406	-0.771 : 0.158
Touchdown shank angle (°)	-0.330	-0.732 : 0.244

599 ** Correlation is significant at the 0.01 level (2-tailed).



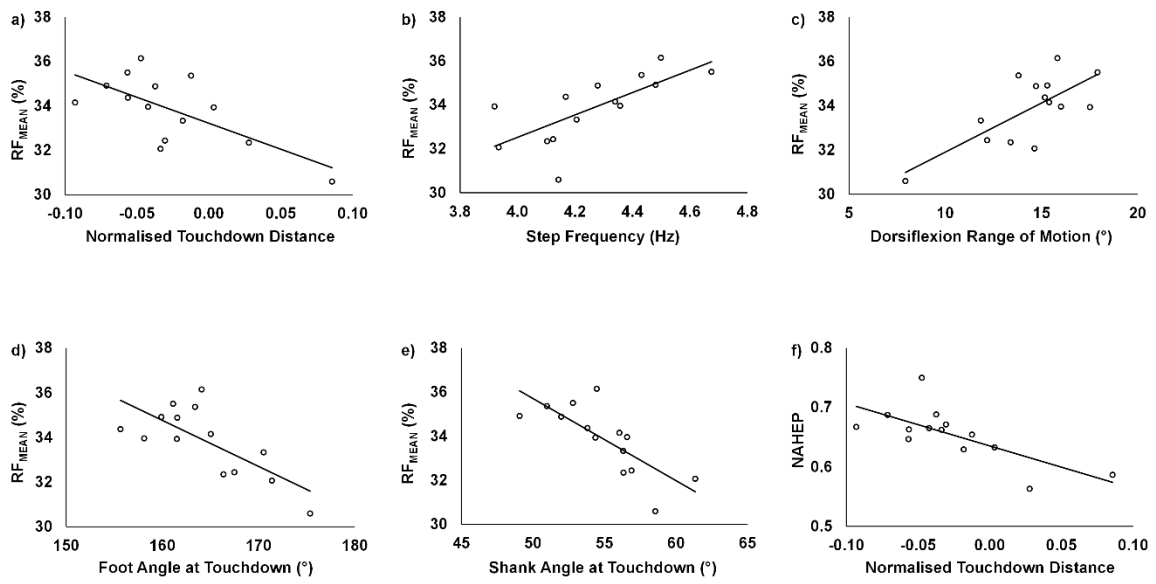
603 **Figure 1.** Angular kinematic conventions for a) the three stance leg joints; and b) the four
604 segments of interest. JC denotes joint centre. Extension/plantar flexion were defined as
605 positive. Segment conventions for the positive direction are displayed on the stance leg,
606 following the conventions of Nagahara et al. (2014a).



608

609 **Figure 2.** Illustration of the typical angular kinematic profiles from the fourth stance phase for
 610 a) ankle angle; b) knee angle; c) hip angle; d) ankle angular velocity; e) knee angular
 611 velocity; and f) hip angular velocity. The discrete variables identified from these time
 612 histories are 1) touchdown angle; 2) dorsiflexion/flexion range of motion; 3) peak
 613 dorsiflexion/flexion angle; 4) plantar flexion/extension range of motion; 5) toe-off angle; 6)
 614 touchdown angular velocity; 7) peak dorsiflexion/flexion angular velocity; 8) peak plantar
 615 flexion/extension angular velocity; and 9) toe-off angular velocity. Note: data from the fourth
 616 stance phase are used to facilitate the illustration of knee flexion during early stance (termed
 617 'Early flexion RoM' in Table 2). Knee flexion during late stance (termed 'Late flexion RoM' in
 618 Table 2) was greatest during the first stance phase (when there was no knee flexion during
 619 early stance) and can be visualised between the two markers on the inset in sub-figure b.

620



621

622 **Figure 3.** Scatter plots for the relationships which were statistically significant (note the
 623 change in dependent variable to NAHEP (normalised average horizontal external power) in
 624 sub-plot f).